Journal of Hazardous Materials 162 (2009) 344–350

Contents lists available at ScienceDirect

Journal of Hazardous Materials

journal homepage: www.elsevier.com/locate/jhazmat

Removal of cationic dye from aqueous solution using jackfruit peel as non-conventional low-cost adsorbent

B.H. Hameed*

School of Chemical Engineering, Engineering Campus, Universiti Sains Malaysia, 14300 Nibong Tebal, Penang, Malaysia

ARTICLE INFO

Article history:
Received 12 February 2008
Received in revised form 11 May 2008
Accepted 12 May 2008
Available online 16 May 2008

Keywords:
Jackfruit peel
Adsorption
Isotherm
Methylene blue
Kinetics

ABSTRACT

This study aimed at investigating the feasibility of using jackfruit peel (JFP), a solid waste, abundantly available in Malaysia, for the adsorption of methylene blue, a cationic dye. Batch adsorption studies were conducted to evaluate the effects of contact time, initial concentration (35–400 mg/L), pH (2–11), and adsorbent dose (0.05–1.20 g) on the removal of dye at temperature of 30 °C. The experimental data were analyzed by the four different types of linearized Langmuir isotherm, the Freundlich isotherm and the Temkin isotherm. The experimental data fitted well with the type 2 Langmuir model with a maximum adsorption capacity of 285.713 mg/g. Pseudo-first and pseudo-second-order kinetics models were tested with the experimental data, and pseudo-second-order kinetics was the best for the adsorption of MB by JFP with coefficients of correlation $R^2 \geq 0.9967$ for all initial MB concentrations studied. The results demonstrated that the JFP is very effective for the adsorption of methylene blue (MB) from aqueous solutions.

1. Introduction

In the textile industry, the modern dyeing processes and machinery are designed for use with synthetic dyes. Dye-containing wastewaters discharged from such industry are well-known pollutants to the receiving bodies in industrial areas. It is therefore imperative to treat textile effluents due to their toxic and esthetic impacts on the receiving water bodies. Many treatment processes have been applied for the removal of dyes from wastewater such as: Fenton process [1], photo/ferrioxalate system [2], photocatalytic and electrochemical combined treatment [3], photocatalytic degradation using UV/TiO_2 [4], sonochemical degradation [5], Fenton-biological treatment scheme [6], biodegradation [7], photo-Fenton processes [8], integrated chemical–biological degradation [9], electrochemical degradation [10] and adsorption process [11,12]. A critical review on current treatment technologies with a proposed alternative was reported by Robinson et al. [13].

Adsorption process using commercial activated carbons is very effective for removal of dyes from wastewater, but its high cost has motivated the search for alternatives and low-cost adsorbents. Such alternatives include: chitosan bead [14], oil palm trunk fiber [15], fly ash [16], dried biomass of Baker's yeast [17], durian (*Durio zibethinus Murray*) peel [18], Guava (*Psidium guajava*) leaf powder [19], chitosan/oil palm ash composite [20], high lime Soma fly ash [21], almond shells [22], pomelo (*Citrus grandis*) peel [23], treated parthenium biomass [24] and broad bean peels [25]. Recently, an extensive list of sorbent literature for dye removal has been compiled by Allen and Koumanova [26].

Jackfruit (*Artocarpus heterophyllus* L.) is a specie of tree of the mulberry family (Moraceae) and is widely grown in Thailand, Indonesia, Myanmar, India, Philippines and Malaysia. Jackfruits usually reach 10–25 kg in weight at maturity [27]. The large sized jackfruits, however, weight as much as 50 kg [28]. About 50% of fruit composed of rind and unfertilized floral parts are usually discarded as waste because they are fibrous [29]. With the increase in production of processed fruit products, the amount of fruit wastes generated is increasing enormously. Jackfruit peel wastes have no economic value and in fact often create a serious problem of disposal for local environments. Thus utilizing jackfruit peel as an alterative and low-cost adsorbent would increase its economic value, help reduce the cost of waste disposal, besides this, the problem of environmental pollution also can be reduced considerably. Therefore, the aim of this study was to investigate the potential of jackfruit peel (JFP), an abundantly available solid waste, as an adsorbent in the removal of methylene blue from aqueous solutions.

* Tel.: +60 4 599 6422.
E-mail address: chbassim@eng.usm.my.

0304-3894/$ – see front matter © 2008 Elsevier B.V. All rights reserved.
doi:10.1016/j.jhazmat.2008.05.045

Table 1
Proximate analysis of jackfruit peels [30]

Material	Weight (%)
Ash	4
Moisture	10
Volatile matter	50
Fixed carbon	36
Total	100.00

2. Materials and methods

2.1. Adsorbate

The methylene blue (MB) used in this work was purchased from Sigma–Aldrich. The MB was chosen in this study because of its known strong adsorption onto solids. The MB (C.I. basic blue 9) used in this study has a molecular weight of 373.90 g/mol, with molecular formula of $C_{16}H_{18}ClN_3S\ 3H_2O$. The maximum wavelength of this dye is 668 nm.

2.2. Adsorbent

The jackfruit peel (JFP) used was collected from the main fruit market of Nibong Tebal, Penang, Malaysia. It was washed thoroughly with distilled water to remove the surface adhered particles. Then it was sliced, spread on trays and oven dried at 70 °C for 48 h. The dried slices were ground and sieved to obtain a particle size range of 0.5–1 mm by collecting the samples which passed through 1-mm sieve and retained on 0.5-mm sieve and the samples were then stored in plastic bottle for further use. No other chemical or physical treatments were used prior to adsorption experiments. Prior to adsorption studies, it was ensured that there was no color produced by the JFP when it was in contact with the dye solution. The proximate analysis of JPF is given in Table 1 [30].

2.3. Equilibrium studies

Adsorption experiments were carried out by adding a fixed amount of sorbent (0.60 g) into a number of 250 mL-stoppered glass Erlenmeyers flasks containing a definite volume (0.20 L in each case) of different initial concentrations (35–400 mg/L) of dye solution without changing pH and temperature 30 °C. The flasks were placed in a thermostatic water-bath shaker and agitation was provided at 130 rpm for 180 min to ensure equilibrium was reached. At time $t = 0$ and equilibrium, the dye concentrations were measured using a double beam UV–vis spectrophotometer (Shimadzu, Model UV 1601, Japan) at 668 nm wavelength. After equilibrium, the sorbent was separated from the dye solution using filtration and the dye concentrations were similarly measured. The amount of adsorption at equilibrium, q_e (mg/g), was calculated by

$$q_e = \frac{(C_0 - C_e)V}{W} \quad (1)$$

where C_0 and C_e (mg/L) are the liquid-phase concentrations of dye at initial and equilibrium, respectively. V (L) is the volume of the solution and W (g) is the mass of dries sorbent used.

The dye removal percentage can be calculated as follows:

$$\text{removal percentage} = \left(\frac{C_0 - C_e}{C_0}\right) \times 100 \quad (2)$$

2.4. Effect of JFP dose

The effect of JFP dose on the amount of MB adsorbed was obtained by adding different amounts of JFP (0.05, 0.10, 0.15, 0.20, 0.40, 0.60, 0.80, 1.00 and 1.20 g) into a number of 250 mL-stoppered glass Erlenmeyers flasks containing a definite volume (0.20 L in each case) of fixed initial concentration (65 mg/L) of dye solution without changing pH (6.5) at temperature 30 °C. The flasks were placed in a thermostated water-bath shaker and agitation was provided at 130 rpm for 180 min. After equilibrium, the sorbent was separated from the dye solution using filtration and the dye concentrations were similarly measured by a double beam UV–vis spectrophotometer.

2.5. Effect of solution pH

In this study, 0.20 L of dye solution of 50 mg/L initial concentration at different pH values (2.0–11.0) was agitated with 0.60 g of JFP in a water-bath shaker at 30 °C. Agitation was made for 180 min at a constant agitation speed of 130 rpm. After equilibrium was established, the sorbent was separated from the dye solution using filtration and the dye concentrations were similarly measured by a double beam UV–vis spectrophotometer. The pH was adjusted with 0.1N NaOH and 0.1N HCl solutions and measured by using a pH meter (Ecoscan, EUTECH Instruments, Singapore).

2.6. Batch kinetic studies

The procedures of kinetic experiments were basically identical to those of equilibrium tests. The aqueous samples were taken at preset time intervals, and the concentrations of dye were similarly measured. All the kinetic experiments were carried out at 30 °C. The amount of sorption at time t, q_t (mg/g), was calculated by

$$q_t = \frac{(C_0 - C_t)V}{W} \quad (3)$$

where C_t (mg/L) is the liquid-phase concentrations of dye at any time.

2.7. Analytical methods

The dye concentrations were monitored by measuring absorbance at 668 nm using a double beam UV–vis spectrophotometer (Shimadzu, Model UV 1601, Japan), after separating the sorbent from the dye solution using filtration. Prior to the measurement, a calibration curve was obtained by using the standard MB solution with the known concentrations.

Table 2
Isotherms and their linearized forms

Isotherm		Linear form	Plot	Ref.
Type 1 Langmuir	$q_e = \frac{q_m K_a C_e}{1+K_a C_e}$	$C_e/q_e = C_e/q_m + 1/K_a q_m$	C_e/q_e vs. C_e	[31]
Type 2 Langmuir		$1/q_e = (1/K_a q_m)(1/C_e) + 1/q_m$	$1/q_e$ vs. $1/C_e$	
Type 3 Langmuir		$q_e = q_m - q_e/K_a C_e$	q_e vs. q_e/C_e	
Type 4 Langmuir		$q_e/C_e = K_a q_m - K_a q_e$	q_e/C_e vs. q_e	
Freundlich	$q_e = K_F C_e^{1/n}$	$\ln q_e = \ln K_F + 1/n \ln C_e$	$\ln q_e$ vs. $\ln C_e$	[32]
Temkin	$q_e = (RT/b)\ln(AC_e)$	$q_e = B \ln A + B \ln C_e$ where $B = RT/b$	q_e vs. $\ln C_e$	[33]

3. Theory

3.1. Equilibrium isotherms

Adsorption isotherm is basically important to describe how solutes interact with adsorbents, and is critical in optimizing the use of adsorbents. Three commonly used isotherms, the Langmuir [31], the Freundlich [32] and the Temkin [33] were employed in the present study. The linearized forms of the three isotherms are shown in Table 2. From Table 2, it was observed that the Langmuir isotherms could be linearized to at least four different types. The Langmuir constants q_m and K_a values can be calculated from the plot between C_e/q_e versus C_e, $1/q_e$ versus $1/C_e$, q_e versus q_e/C_e, and q_e/C_e versus q_e for types 1, type 2, type 3 and type 4 linearized Langmuir isotherms, respectively. q_m (mg/g) and K_a (L/mg) are Langmuir constants related to adsorption capacity and energy of adsorption, respectively.

Similarly the Freundlich isotherm constants K_F and n which are indicators of adsorption capacity and adsorption intensity, respectively [34] can be calculated from the plot of $\ln(q_e)$ versus $\ln(C_e)$. The Temkin isotherm [33] has generally been applied in the form shown in Table 2. Therefore, by plotting q_e versus $\ln C_e$ aids the determination of the constants A and B. B is the Temkin constant related to heat of sorption (J/mol); A is the Temkin isotherm constant (L/g), R the gas constant (8.314 J/mol. K) and T is the absolute temperature (K).

3.2. Adsorption kinetics

The Lagergren's pseudo-first-order model (Eq. (4)) [35] and pseudo-second-order model (Eq. (5)) [36] have been widely used to predict sorption kinetics. The pseudo-first-order equation is generally applicable over the initial stage of the adsorption processes whereas the pseudo-second-order equation predicts the behavior over the whole range of adsorption. These two models were used in this study to fit the experimental data:

$$\log(q_e - q_t) = \log q_e - \left(\frac{k_1}{2.303}\right) t \quad (4)$$

$$\frac{t}{q_t} = \frac{1}{k_2 q_e^2} + \left(\frac{1}{q_e}\right) t \quad (5)$$

where k_1 (1/min) is the rate constant of pseudo-first-order adsorption, k_2 (g/mg min) is the rate constant of pseudo-second-order adsorption.

3.3. Intraparticle diffusion model

In order to investigate the mechanism of the MB adsorption onto JFP, intraparticle diffusion based mechanism has been studied. The most commonly used technique for identifying the mechanism involved in the adsorption process is by fitting an intraparticle diffusion plot. It is an empirically found functional relationship, common to the most adsorption processes, where uptake varies almost proportionally with $t^{1/2}$ rather than with the contact time t. According to the theory proposed by Weber and Morris [37]:

$$q_t = k_{pi} t^{1/2} + C_i \quad (6)$$

where k_{pi} (mg/g min$^{1/2}$), the rate parameter of stage i, is obtained from the slope of the straight line of q_t versus $t^{1/2}$ whereas C_i is the intercept of the plot which gives an idea about the thickness of boundary layer.

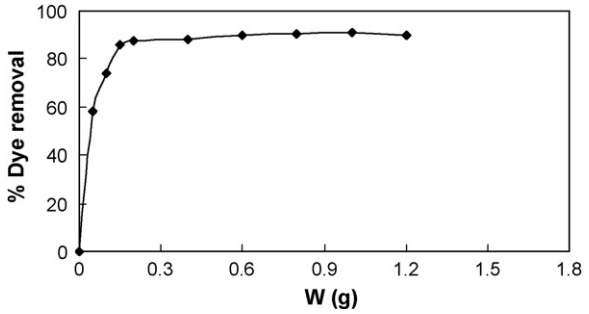

Fig. 1. Effect of adsorbent dosage on the adsorption of MB on JFP (T = 30 °C, V = 0.20 L; pH 6.5; C_0 = 65 mg/L, stirring rate = 130 rpm).

4. Results and discussion

4.1. Effect of adsorbent dose on dye adsorption

In order to investigate the effect of adsorbent dose (g) on dye adsorption, experiments were conducted at initial dye concentration of 65 mg/L, while the amount of adsorbent added was varied. Fig. 1 shows the effect of adsorbent dose on the % removal of MB. At equilibrium time, the % removal increased from 58.20% to 89.80% for an increase in JFP dose from 0.05 to 0.60 g. The increase in % color removal was due to the increase in the available sorption surface and sites. The increase in % color removal with increase in adsorbent mass is in agreement with the report of the sorption of methylene blue onto fly ash [38].

4.2. Effect of solution pH on dye uptake

The effect of initial pH on equilibrium capacity of JFP was studied at 50 mg/L initial MB concentration and at 30 °C. Fig. 2 shows that the sorption of MB was minimum at the initial pH 2 and increased with pH up to 4.0 and then remained nearly constant over the initial pH ranges of 4–10, and thereafter started to decrease. The observed low adsorption rate of MB on the JFP at pH < 4 may be because the surface charge become positively charged, thus making (H^+) ions compete effectively with dye cations causing a decrease in the amount of dye adsorbed. A similar behavior was observed for methylene blue adsorption on wheat shells [39].

4.3. Effect of contact time and initial concentration

The adsorption of MB on JFP was studied at different initial MB concentrations (35–400 mg/L). Fig. 3 shows the result for effect of initial concentration on adsorption of MB onto JFP at 30 °C. It

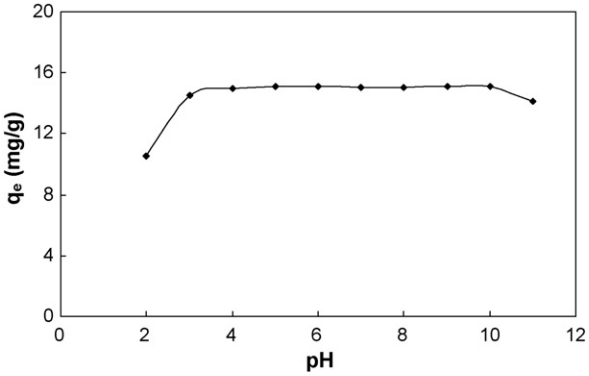

Fig. 2. Effect of pH on equilibrium uptake of MB (W = 0.60 g; V = 0.20 L; C_0 = 50 mg/L, T = 30 °C; stirring rate = 130 rpm).

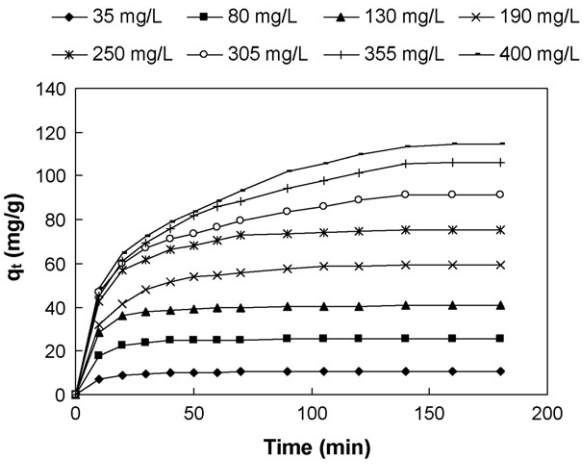

Fig. 3. Effect of initial concentration and contact time on MB adsorption (W = 0.60 g; V = 0.20 L; T = 30 °C; pH 6.5; stirring rate = 130 rpm).

was observed that dye uptake was rapid for the first 30 min, and thereafter proceeded at a slower rate and finally attains saturation. Fig. 3 indicates that an increase in initial MB concentration leads to increase in the adsorption of MB on JFP. The equilibrium adsorption increases from 10.60 to 114.69 mg/g, with increase in the initial MB concentration from 35 to 400 mg/L. As the initial MB concentration increased from 35 to 400 mg/L the equilibrium removal of MB decreased from 93.33% to 86%.

The adsorption of MB on JFP was found to reach equilibrium in less than 60 min for MB solutions with lower initial concentration (35–80 mg/L), while at higher initial MB concentration (130–400 mg/L), the time necessary to reach equilibrium was 120 min. However, the experimental data were measured at 180 min to be sure that full equilibrium was attained. Data on the adsorption kinetics of MB by various adsorbent have shown a similar range of adsorption rates. Han et al. [40] studied the adsorption of methylene blue on fallen phoenix tree's leaves and reported that the equilibrium was reached in 150 min.

4.4. Isotherm analysis

Several mathematical models can be used to describe experimental data of adsorption isotherms. In this work, the equilibrium data for MB on JFP were modeled with the Langmuir (four linearized expressions), Freundlich and Temkin models. The details of the four types of linearized Langmuir isotherms are given in Table 2 and their respective plots are shown in Fig. 4. The values of the Langmuir constants obtained in this study are presented in Table 3. The coefficient of correlation (R^2 = 0.9939) obtained from type 2 Langmuir expression indicates that type 2 Langmuir expressions provided a better fit for the experimental data of MB on JFP.

The essential characteristics of the Langmuir isotherm can be expressed in terms of a dimensionless constant separation factor R_L that is given by the following equation [41]:

$$R_L = \frac{1}{1 + K_a C_0} \quad (7)$$

where C_0 (mg/L) is the highest initial concentration of adsorbate and K_a (L/mg) is Langmuir constant. The value of R_L indicates the shape of the isotherm to be either unfavorable ($R_L > 1$), linear ($R_L = 1$), favorable ($0 < R_L < 1$), or irreversible ($R_L = 0$). The R_L value for the adsorption of MB onto JFP was 0.1269, indicating that the adsorption is a favorable process.

The equilibrium data were further analyzed using the linearized form of Freundlich isotherm, by plotting $\ln q_e$ versus $\ln C_e$ (Fig. 5).

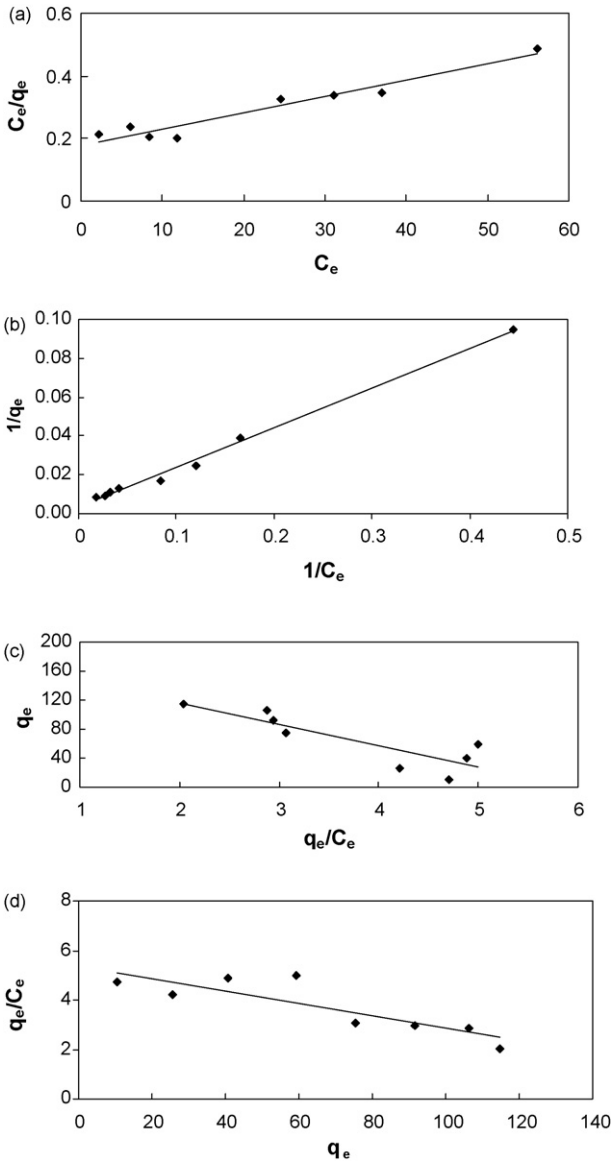

Fig. 4. Langmuir isotherm of MB on JFP at 30 °C: (a) type 1 Langmuir; (b) type 2 Langmuir; (c) type 3 Langmuir; (d) type 4 Langmuir.

The calculated Freundlich isotherm constants and the corresponding coefficient of correlation values are shown in Table 3. The coefficient of correlation was high (R^2 = 0.9576) showing a good linearity. The result shows that the value of n is greater than unity (n = 1.343) indicating that the dye is favorably adsorbed on JFP. The magnitude of Freundlich constant (n = 1.343) indicates easy uptake of MB from aqueous solution.

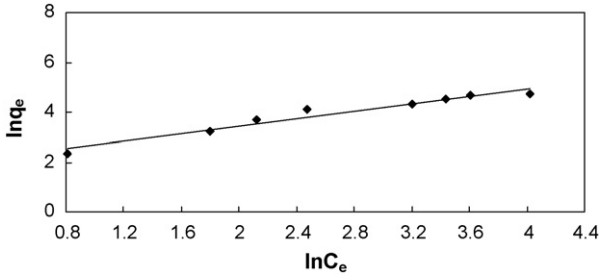

Fig. 5. Freundlich adsorption isotherm of MB on JFP.

Table 3
Isotherm parameters for removal of MB on JFP

Isotherm	Linear form	Parameters	Values
Langmuir	Type 1	q_m (mg/g)	192.308
		K_a (L/mg)	0.0291
		R^2	0.9375
Langmuir	Type 2	q_m (mg/g)	285.713
		K_a (L/mg)	0.0172
		R^2	0.9939
Langmuir	Type 3	q_m (mg/g)	173.410
		K_a (L/mg)	0.0344
		R^2	0.7278
Langmuir	Type 4	q_m (mg/g)	213.506
		K_a (L/mg)	0.0251
		R^2	0.7278
Freundlich		K_F	7.067
		n	1.343
		R^2	0.9576
Temkin		A (l/g)	0.452
		B	34.622
		R^2	0.9640

Table 4
Comparison of adsorption capacities of various adsorbents for methylene blue

Adsorbent	Maximum adsorption capacity (mg/g)	Ref.
Jackfruit peels	285.713	This work
Yellow passion fruit waste	44.70	[43]
Luffa cylindrica fibers	47	[42]
Guava (*Psidium guajava*) leaf powder	185.2	[19]
Dehydrated peanut hull	123.5	[44]
Coffee husks	90.09	[45]
Activated carbon prepared from a renewable bio-plant of *Euphorbia rigida*	109.98	[46]
Activated carbon prepared from durian shell	289.26	[47]
Coir pith carbon	5.87	[48]
Activated carbon prepared from rattan sawdust	294.14	[12]
Bamboo-based-activated carbon	454.2	[49]
Oil palm fiber-activated carbon	277.78	[11]
Activated carbon prepared from oil palm shell	243.90	[50]

The adsorption data for MB on JFP were subjected to regression analysis to fit the Temkin isotherm model (Fig. 6). The parameters of Temkin model as well as the correlation coefficient are listed in Table 3. The coefficient of correlation was high ($R^2 = 0.9640$) showing a good linearity. From Table 3, it can be concluded the type 2 Langmuir was more suitable for the experimental data than other isotherms because of the higher value of correlation coefficient ($R^2 = 0.9939$). This indicates that the adsorption of MB on JFP takes place as monolayer adsorption on a surface that is homogenous in adsorption affinity. A similar result was reported for the adsorption of MB on *Luffa cylindrica* fibers [42]. Table 3 indicates that the computed maximum monolayer adsorption capacity q_m of JFP was relatively large (285.713 mg/g). The comparison of adsorption capacity of the JFP with other adsorbents in literature [11,12,42–50] for the adsorption of MB is presented in Table 4. It can be seen that the JFP is more effective for this purpose even when compared with some of the activated carbons reported in the literature [11,46,50].

4.5. Adsorption kinetics

For evaluating the adsorption kinetics of MB, the pseudo-first-order and pseudo-second-order kinetic models were used to fit the experimental data. Using Eq. (4), a $\log(q_e - q_t)$ versus t was plotted at different MB concentrations (Fig. 7). The pseudo-first-order model data do not fall on straight lines for most initial concentrations indicating that this model is less appropriate. The Lagergren first-order rate constant (k_1) and $q_{e,cal}$ determined from the model are presented in Table 5 along with the corresponding correlation coefficients.

The experimental kinetic data were further analyzed using the pseudo-second-order model. By plotting t/q_t against t for different initial MB concentration (Fig. 8), a straight line was obtained in all cases and using Eq. (5) the second-order rate constant (k_2) and q_e values were determined from the plots. The values of correlation coefficient were very high ($R^2 > 0.9967$) and the theoretical $q_{e,cal}$ values obtained from this model were closer to the experimental $q_{e,exp}$ values at different initial MB concentrations (Table 5). It is important to note that for the pseudo-first-order model, the correlation coefficient obtained in this study, $R^2 \leq 0.9834$ at different initial MB concentrations, which is lower as compared to the correlation coefficient obtained from the pseudo-second-order model. Moreover, from Table 5, it can be seen that the experimental values of $q_{e,exp}$ are not in good agreement with the theoretical values calculated ($q_{e,cal}$) from the pseudo-first-order equation. Therefore, it can be concluded that the pseudo-second-order kinetic model provided a better correlation for the adsorption of MB on JFP at different initial MB concentrations compared to the pseudo-first-order model. A similar result was reported for the adsorption of MB on *L. cylindrica* fibers [42], adsorption of MB from aqueous solution by dehydrated wheat bran carbon [51] and adsorption of MB on Guava (*P. guajava*) leaf powder [19].

The first-order and pseudo-second-order kinetic models could not identify the diffusion mechanism. Thus the kinetic results were then analyzed by using the intraparticle diffusion model. Weber and Moris plot [52] (q_t versus $t^{0.5}$) was used to investigate intra-

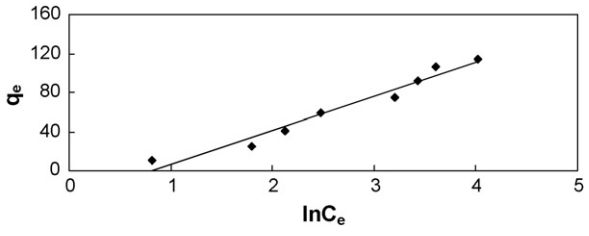

Fig. 6. Temkin adsorption isotherm of MB on JFP.

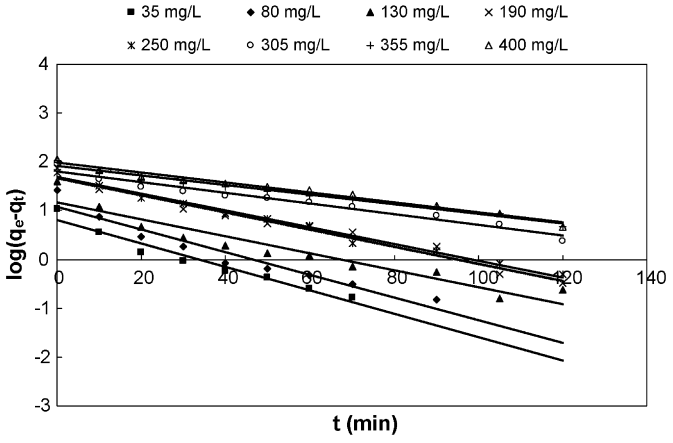

Fig. 7. Pseudo-first-order kinetic for adsorption of MB on JFP.

Table 5
Comparison of the pseudo-first-order and pseudo-second-order adsorption rate constants, and calculated and experimental q_e values for different initial MB concentrations

Initial conc. (mg/L)	$q_{e,exp}$ (mg/g)	Pseudo-first-order kinetic model			Pseudo-second-order kinetic model		
		k_1 (1/min)	$q_{e,cal}$ (mg/g)	R^2	k_2 (g/mg min) 10^4	$q_{e,cal}$ (mg/g)	R^2
35	10.583	0.0554	6.362	0.9565	341.025	10.787	0.9996
80	25.483	0.0537	12.045	0.9378	35.555	24.096	0.9977
130	40.703	0.0398	14.508	0.9066	21.572	38.610	0.9979
190	59.338	0.0387	42.355	0.9807	10.301	58.139	0.9978
250	75.280	0.0396	49.272	0.9834	8.727	73.529	0.9978
305	91.432	0.0758	533.330	0.7704	5.062	91.743	0.9976
355	106.306	0.0559	362.660	0.6882	3.575	109.890	0.9975
400	114.690	0.3685	166.533	0.8332	3.079	120.481	0.9967

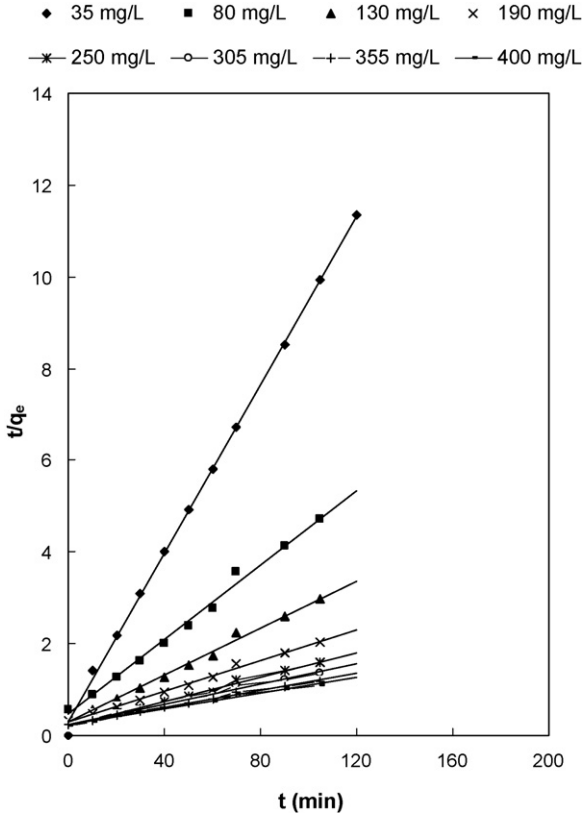

Fig. 8. Pseudo-second-order kinetic for adsorption of MB on JFP.

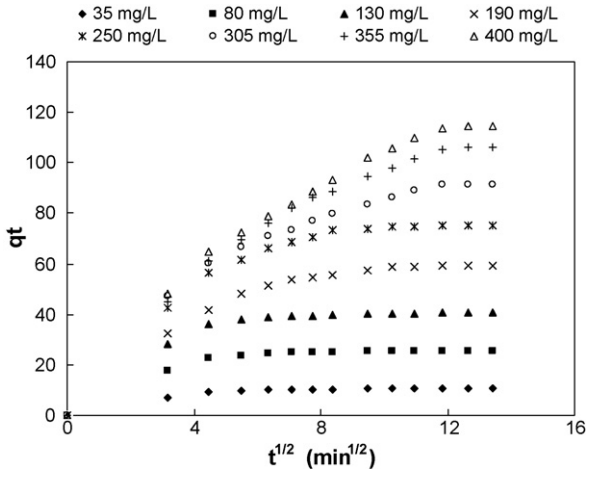

Fig. 9. Intraparticle diffusion plot for adsorption of MB on JFP for different initial MB concentrations.

particle diffusion mechanism (Fig. 9). If the intraparticle diffusion was the only rate-controlling step, the plot passed through the origin; if not, the boundary layer diffusion controlled the adsorption to some degree [53]. As seen from Fig. 9, the plots were not linear over the whole time range, implying that more than one process affected the adsorption. A similar behavior was reported for the methylene blue sorption onto palm kernel fiber [54].

5. Conclusions

The present work shows that JFP can be used as an adsorbent for the removal of methylene blue dye from aqueous solutions. The amount of dye adsorbed was found to vary with initial methylene blue concentration and contact time. The type 2 Langmuir adsorption isotherms was found to provide the best fit to the experimental data with maximum adsorption capacity of 285.713 mg/g. The adsorption kinetics can be predicted by pseudo-second-order kinetic. The results of the present investigation indicate that the JFP has a potential for use in removing methylene blue from aqueous solutions.

Acknowledgments

The authors acknowledge the research grant provided by the Universiti Sains Malaysia under the Research University (RU) Scheme (Project No.: 1001/PJKIMIA/814005).

References

[1] M.A. Behnajady, N. Modirshahla, F. Ghanbary, A kinetic model for the decolorization of C.I. Acid Yellow 23 by Fenton process, J. Hazard. Mater. 148 (2007) 98–102.
[2] Y.H. Huang, S.T. Tsai, Y.F. Huang, C.Y. Chen, Degradation of commercial azo dye reactive Black B in photo/ferrioxalate system, J. Hazard. Mater. 140 (2007) 382–388.
[3] M.G. Neelavannan, M. Revathi, C. Ahmed Basha, Photocatalytic and electrochemical combined treatment of textile wash water, J. Hazard. Mater. 149 (2007) 371–378.
[4] M.R. Sohrabi, M. Ghavami, Photocatalytic degradation of Direct Red 23 dye using UV/TiO_2: effect of operational parameters, J. Hazard. Mater. 153 (2008) 1235–1239.
[5] M. Abbasi, N.R. Asl, Sonochemical degradation of Basic Blue 41 dye assisted by nanoTiO_2 and H_2O_2, J. Hazard. Mater. 153 (2008) 942–947.
[6] B. Lodha, S. Chaudhari, Optimization of Fenton-biological treatment scheme for the treatment of aqueous dye solutions, J. Hazard. Mater. 148 (2007) 459–466.
[7] N. Daneshvar, A.R. Khataee, M.H. Rasoulifard, M. Pourhassan, Biodegradation of dye solution containing Malachite Green: optimization of effective parameters using Taguchi method, J. Hazard. Mater. 143 (2007) 214–219.
[8] J. García-Montaño, N. Ruiz, I. Muñoz, X. Domènech, J.A. García-Hortal, F. Torrades, J. Peral, Environmental assessment of different photo-Fenton approaches for commercial reactive dye removal, J. Hazard. Mater. 138 (2006) 218–225.
[9] G. Sudarjanto, B. Keller-Lehmann, J. Keller, Optimization of integrated chemical–biological degradation of a reactive azo dye using response surface methodology, J. Hazard. Mater. 138 (2006) 160–168.
[10] L. Fan, Y. Zhou, W. Yang, G. Chen, F. Yang, Electrochemical degradation of aqueous solution of Amaranth azo dye on ACF under potentiostatic model, Dyes Pigments 76 (2008) 440–446.

[11] I.A.W. Tan, B.H. Hameed, A.L. Ahmad, Equilibrium and kinetic studies on basic dye adsorption by oil palm fibre activated carbon, Chem. Eng. J. 127 (2007) 111–119.
[12] B.H. Hameed, A.L. Ahmad, K.N.A. Latiff, Adsorption of basic dye (methylene blue) onto activated carbon prepared from rattan sawdust, Dyes Pigments 75 (2007) 143–149.
[13] T. Robinson, G. McMullan, R. Marchant, P. Nigam, Remediation of dyes in textile effluent: a critical review on current treatment technologies with a proposed alternative, Bioresour. Technol. 77 (2001) 247–255.
[14] Z. Bekçi, C. Özveri, Y. Seki, K. Yurdakoç, Sorption of malachite green on chitosan bead, J. Hazard. Mater. 154 (2008) 254–261.
[15] B.H. Hameed, M.I. El-Khaiary, Batch removal of malachite green from aqueous solutions by adsorption on oil palm trunk fibre: equilibrium isotherms and kinetic studies, J. Hazard. Mater. 154 (2008) 237–244.
[16] P. Pengthamkeerati, T. Satapanajaru, O. Singchan, Sorption of reactive dye from aqueous solution on biomass fly ash, J. Hazard. Mater. 153 (2008) 1149–1156.
[17] J.Y. Farah, N.S. El-Gendy, L.A. Farahat, Biosorption of Astrazone Blue basic dye from an aqueous solution using dried biomass of Baker's yeast, J. Hazard. Mater. 148 (2007) 402–408.
[18] B.H. Hameed, H. Hakimi, Utilization of durian (*Durio zibethinus Murray*) peel as low cost sorbent for the removal of acid dye from aqueous solutions, Biochem. Eng. J. 39 (2008) 338–343.
[19] V. Ponnusami, S. Vikram, S.N. Srivastava, Guava (*Psidium guajava*) leaf powder: novel adsorbent for removal of methylene blue from aqueous solutions, J. Hazard. Mater. 152 (2008) 276–286.
[20] M. Hasan, A.L. Ahmad, B.H. Hameed, Adsorption of reactive dye onto cross-linked chitosan/oil palm ash composite beads, Chem. Eng. J. 136 (2008) 164–172.
[21] Z. Eren, F.N. Acar, Equilibrium and kinetic mechanism for Reactive Black 5 sorption onto high lime Soma fly ash, J. Hazard. Mater. 143 (2007) 226–232.
[22] F.D. Ardejani, K. Badii, N.Y. Limaee, S.Z. Shafaei, A.R. Mirhabibi, Adsorption of Direct Red 80 dye from aqueous solution onto almond shells: effect of pH, initial concentration and shell type, J. Hazard. Mater. 151 (2008) 730–737.
[23] B.H. Hameed, D.K. Mahmoud, A.L. Ahmad, Sorption of basic dye from aqueous solution by Pomelo (*Citrus grandis*) peel in a batch system, Colloids Surf. A: Physicochem. Eng. Aspects 316 (2008) 78–84.
[24] H. Lata, S. Mor, V.K. Garg, R.K. Gupta, Removal of a dye from simulated wastewater by adsorption using treated parthenium biomass, J. Hazard. Mater. 153 (2008) 213–220.
[25] B.H. Hameed, M.I. El-Khaiary, Sorption kinetics and isotherm studies of a cationic dye using agricultural waste: broad bean peels, J. Hazard. Mater. 154 (2008) 639–648.
[26] S.J. Allen, B. Koumanova, Decolourisation of water/wastewater using adsorption, J. Univ. Chem. Technol. Metal. 40 (2005) 175–192.
[27] A.K.M.M. Rahman, H. Enamal, A.J. Mian, A. Chesson, Microscopic and chemical changes occurring during the ripening of two forms of jackfruit (*Artocarpus heterophyllus* L.), Food Chem. 52 (1995) 405–410.
[28] Y. Selvaraj, D.K. Pal, Biochemical changes during the ripening of jackfruit (*Artocarpus heterophyllus* L.), J. Food Sci. Technol. 26 (1989) 304–307.
[29] P.J. John, P. Narasimham, Processing and evaluation of carbonated beverage from Jackfruit waste (*Artocarpus heterophyllus*), J. Food Proc. Preserv. 16 (1993) 373–380.
[30] D. Prahas, Y. Kartika, N. Indraswati, S. Ismadji, Activated carbon from jackfruit peel waste by H_3PO_4 chemical activation: pore structure and surface chemistry characterization, Chem. Eng. J. 140 (2008) 32–42.
[31] I. Langmuir, The constitution and fundamental properties of solids and liquids, J. Am. Chem. Soc. 38 (11) (1916) 2221–2295.
[32] H.M.F. Freundlich, Over the adsorption in solution, J Phys. Chem. 57 (1906) 385–470.
[33] M.J. Temkin, V. Pyzhev, Recent modifications to Langmuir Isotherms, Acta Physiochim. USSR 12 (1940) 217–222.
[34] Y.S. Ho, G. McKay, Sorption of dye from aqueous solution by peat, Chem. Eng. J. 70 (1998) 115–124.
[35] S. Lagergren, About the theory of so-called adsorption of soluble substances, K. Sven Vetenskapsakad. Handl. 24 (4) (1898) 1–39.
[36] Y.S. Ho, G. McKay, Sorption of dye from aqueous solution by peat, Chem. Eng. J. 70 (1978) 115–124.
[37] W.J. Weber, J.C. Morris, Kinetics of adsorption on carbon from solution, J. Sanitary Eng. Div. Proceed. Am. Soc. Civil Eng. 89 (1963) 31–59.
[38] K.V. Kumar, V. Ramamurthi, S. Sivanesan, Modeling the mechanism involved during the sorption of methylene blue onto fly ash, J. Colloid Interf. Sci. 284 (2005) 14–21.
[39] Y. Bulut, H. Aydın, A kinetics and thermodynamics study of methylene blue adsorption on wheat shells, Desalination 194 (2006) 259–267.
[40] R. Han, W. Zou, W. Yu, S. Cheng, Y. Wang, J. Shi, Biosorption of methylene blue from aqueous solution by fallen phoenix tree's leaves, J. Hazard. Mater. 141 (2007) 156–162.
[41] K.R. Hall, L.C. Eagleton, A. Acrivos, T. Vermeulen, Pore- and solid-diffusion kinetics in fixed-bed adsorption under constant-pattern conditions, I&EC Fundam. 5 (1966) 212–223.
[42] H. Demir, A. Top, D. Balköse, S. Ülkü, Dye adsorption behavior of *Luffa cylindrica* fibers, J. Hazard. Mater. 153 (2008) 389–394.
[43] F.A. Pavan, E.C. Lima, S.L.P. Dias, A.C. Mazzocato, Methylene blue biosorption from aqueous solutions by yellow passion fruit waste, J. Hazard. Mater. 150 (2008) 703–712.
[44] D. Özer, G. Dursun, A. Özer, Methylene blue adsorption from aqueous solution by dehydrated peanut hull, J. Hazard. Mater. 144 (2007) 171–179.
[45] L.S. Oliveira, A.S. Franca, T.M. Alves, S.D.F. Rocha, Evaluation of untreated coffee husks as potential biosorbents for treatment of dye contaminated waters, J. Hazard. Mater. 155 (2008) 507–512.
[46] Ö. Gerçel, A. Özcan, A.S. Özcan, H.F. Gerçel, Preparation of activated carbon from a renewable bio-plant of *Euphorbia rigida* by H_2SO_4 activation and its adsorption behavior in aqueous solutions, Appl. Surf. Sci. 253 (2007) 4843–4852.
[47] T.C. Chandra, M.M. Mirna, Y. Sudaryanto, S. Ismadji, Adsorption of basic dye onto activated carbon prepared from durian shell: studies of adsorption equilibrium and kinetics, Chem. Eng. J. 127 (2007) 121–129.
[48] D. Kavitha, C. Namasivayam, Experimental and kinetic studies on methylene blue adsorption by coir pith carbon, Bioresour. Technol. 98 (2007) 14–21.
[49] B.H. Hameed, A.T.M. Din, A.L. Ahmad, Adsorption of methylene blue onto bamboo-based activated carbon: kinetics and equilibrium studies, J. Hazard. Mater. 141 (2007) 819–825.
[50] I.A.W. Tan, A.L. Ahmad, B.H. Hameed, Adsorption of basic dye using activated carbon prepared from oil palm shell: batch and fixed bed studies, Desalination 225 (2008) 13–28.
[51] A. Özer, G. Dursun, Removal of methylene blue from aqueous solution by dehydrated wheat bran carbon, J. Hazard. Mater. 146 (2007) 262–269.
[52] W.J. Weber Jr., J.C. Morris, Kinetics of adsorption on carbon from solution, J. Sanitary Eng. Div. Proceed. Am. Soc. Civil Eng. 89 (1963) 31–59.
[53] W.H. Cheung, Y.S. Szeto, G. McKay, Intraparticle diffusion processes during acid dye adsorption onto chitosan, Bioresour. Technol. 98 (2007) 2897–2904.
[54] A.E. Ofomaja, Kinetics and mechanism of methylene blue sorption onto palm kernel fibre, Process Biochem. 42 (2007) 16–24.